DOI: 10.1002/ejic.200600151

σ-Silane Ruthenium Complexes: The Crucial Role of Secondary Interactions

Sébastien Lachaize[a] and Sylviane Sabo-Etienne*[a]

Keywords: σ-Complexes / Ruthenium / Silanes / Hydrides / Coordination modes / Intramolecular interactions / Oxidative addition / Hypervalent compounds

The bonding coordination mode of various silanes to ruthenium complexes is discussed on the basis of a detailed analysis of NMR, IR, X-ray and DFT data. It is now more and more obvious that a continuum exists between the two extreme situations, i.e. formation of a σ-silane complex or Si–H bond breaking leading to oxidative addition. Within this continuum, secondary interactions involving Si and H play a significant role, in particular for the stabilization of unusual structures or as intermediates in exchange processes. Here, we highlight the criteria allowing the best description of the different bonding modes.

Introduction

A σ-complex is defined by the coordination of an H–E (E = H, Si, B, C...) bond to a metal center, a three center-two electron bond. "True" σ-complexes display no intramolecular interaction as the one found in the related family of agostic complexes. σ-complexes are now well recognized, and their properties have been reviewed in an excellent monograph by G. Kubas.[1] A parallel is often made with the Chatt–Dewar and Duncanson model, thus involving two components, σ-donation and back-donation (see Figure 1). Among the four main classes of σ-complexes (σ-dihydrogen,[1–3] σ-silane,[1,4–6] σ-borane[1,7] and σ-alcane[1,8,9]) σ-dihydrogen complexes are the most numerous and also the most documented. One of the main reasons is that two identical atoms are involved in the σ-coordination, whereas the situation is much more complex for the other cases. The substituents on the E atom have a tremendous impact, as steric and electronic effects can tune the σ-coordination. We will see in this review that in silane chemistry, the situation is quite complex, in particular as a result of the hyperval-

[a] Laboratoire de Chimie de Coordination du CNRS,
205 route de Narbonne, 31077 Toulouse Cedex 04, France
E-mail: sabo@lcc-toulouse.fr

Sylviane Sabo-Etienne was born in France in 1956. She received her "Doctorat d'Etat" from the Université Paul Sabatier, Toulouse, in 1984, under the supervision of the late Professor Danièle Gervais, in the field of heterobimetallic complexes. In 1985, she moved to the Université de Bretagne Occidentale in Brest, to work as "Chargée de Recherche" in Prof. Hervé des Abbayes' group in the field of carbonylation. After a year working with Prof. Maurice Brookhart (Chapel Hill, USA) as a NSF-CNRS research associate, on acrylate dimerization, she returned to Toulouse to the Laboratoire de Chimie de Coordination to work in collaboration with Dr. Bruno Chaudret on polyhydride chemistry. She was promoted to the position of "Directrice de Recherche" in 1997. Her research interests deal with various aspects of coordination chemistry, organometallic chemistry and catalysis with some emphasis on the chemistry of σ-complexes. Silane and borane activation, role of secondary interactions, catalytic studies in the field of hydrogenation and C–X bond breaking and formation (X = B, C, Si, S, CN...), hydrogen transfer and C–H activation, assembly of novel functional groups, are present research topics.

Sébastien Lachaize was born in France in 1976. After graduating from the Ecole Normale Supérieure, Lyon, in 2001, he moved to Toulouse in the group of Dr. Bruno Chaudret at the Laboratoire de Chimie de Coordination. He received his PhD from the Université Paul Sabatier, Toulouse, in 2004 under the supervision of Dr Sylviane Sabo-Etienne working on σ H–E (E = H, Si and B) bond activation by ruthenium complexes. After one year as a postdoctoral fellow in Rochester, NY, USA, working with Prof. William D. Jones on C–CN bond activation, he came back to Toulouse in September 2005. He is currently a "Attaché Temporaire d'Enseignement et de Recherche" at the Institut National des Sciences Appliquées. His current research interests concern the synthesis of metallic nanoparticles using an organometallic route, with special focus on fundamental aspects of the nucleation-growth mechanism, control of the nanoparticle physical properties, and development of new applications.

MICROREVIEWS: This feature introduces the readers to the authors' research through a concise overview of the selected topic. Reference to important work from others in the field is included.

ence properties of silicon.[10] It is first interesting to compare the coordination of a dihydrogen and of a silane ligand to a metal center. The silane ligand imposes a dissymmetry in the coordination mode, due to the difference in size and electronegativity of the two elements. The Si–H bond is more basic than the H–H bond, and thus is a better σ-donor. Moreover, the Si–H bond is also a better π acceptor, as the σ*(Si–H) orbital is lower in energy than the σ*(H–H) orbital (dissociation energy for the Si–H bond in the range 350–430 kJ·mol^{-1} vs. 435 kJ·mol^{-1} for H_2). When a competition between σ-dihydrogen or σ-silane coordination exists, σ-silane coordination is thus favoured. By comparison to the dihydrogen complexes, the σ-silanes are generally more advanced in the process of oxidative addition, thanks again to a better back donation. For this reason, it is often difficult to discriminate a σ-silane coordination from a hydrido(silyl) formulation.[11] σ-Silane complexes exist for a wide variety of metals, but this review will focus on ruthenium complexes, a metal of choice to act as catalyst precursor for several processes such as hydrosilylation, dehydrosilylative coupling of alkenes, and dehydrogenative polymerisation.[12,13] Moreover, polyhydride ruthenium complexes offer to analyze a wide range of situations. Indeed, a hydrogen atom can be coordinated to the metal as a classical hydride, involved in a σ-coordination (σ-dihydrogen or σ-silane), or in a secondary interaction with a silicon atom. We will in particular highlight the role of additional interactions in the coordination sphere of a metal, as they play a major role for the stabilization of silane complexes and are involved in most of the exchange processes that are often present in these highly dynamic systems.[14]

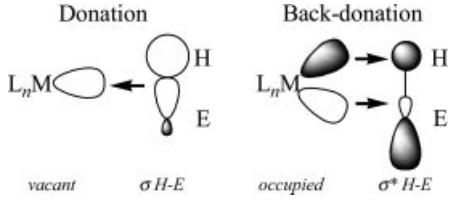

Figure 1. Bonding interactions in a σ-complex.

However, before presenting the different complexes, we would like to give some essential and fairly general features to illustrate the main issues in relation with the degree of activation of the Si–H bond. Between the two extreme situations, formation of a σ-silane complex or Si–H bond breaking and formation of a hydrido(silyl) complex, the Si–H bond activation can be viewed as a continuum (Figure 2). As a consequence, it is extremely difficult to establish the boundaries between the extremes, especially when other hydrogen atoms are present in the coordination sphere of the metal. In such a case, thanks to the tendency of Si to be hypervalent, additional interactions can be established. We have introduced the term *SISHA* to shorten the rather long quotation: *S*econdary *I*nteraction between a *S*ilicon and a *H*ydrogen *A*tom.[14] These interactions play an important role both in the stabilization of unusual geometries and in the exchange processes occurring in polyhydride species. At this point, it is important to remember the preference of ruthenium for oxidation state (II) vs. (IV) and that polyhydride ruthenium chemistry is dominated by σ-ligand coordination.

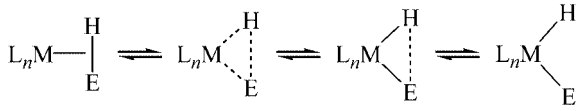

Figure 2. E–H bond activation: a continuum between the σ-complex and the product of oxidative addition.

Multinuclear NMR studies are particularly useful and give key information on the exchange processes and the activation of the Si–H bond. ^{1}H chemical shift values are not a very useful parameter, as those for classical hydrides and hydrogen atoms involved in a σ-bond fall in the same range. A similar situation is found for ^{29}Si chemical shift values of the corresponding silane or silyl complexes. Coupling constant values have been extensively used in particular to discriminate the two extremes, σ-silane complex and oxidative addition product. However, as we will detail below (see *primary silane* section) cautious must be taken in particular for values between 20 and 50 Hz, depending on the substituents on the silicon and in presence of fast exchange processes, which is unfortunately the case for many systems. Activation of the Si–H bond can also be monitored by IR. It is easy to follow the addition of a silane to a transition-metal complex by checking the disappearance of the stretching Si–H bond in the free silane (around 2100–2150 cm^{-1}). It is much more difficult to identify the corresponding band in a σ-silane complex (around 1000 cm^{-1}) due to extensive mixing of vibrational motions and overlap with some bands of other ligands. However, in many cases, a broad and rather intense band can be observed in the range 1650–1800 cm^{-1}, identified as an antisymmetric stretch of the activated Ru–H bond, with H still coordinated to Si. X-ray analysis and DFT calculations are very informative for the identification of σ-bonds and secondary interactions. It is worth noting that X-ray data are now more and more reliable for hydrogen location.[15] Low temperature and high quality measurements are of course required, and comparison with DFT data is very useful. Key parameters, as we will see below, are not only the Si–H distances, but also the Ru–Si distances. The Ru–Si distance within a series of compounds diminishes as the activation of the Si–H bond increases. For Si–H distances of typically 1.7–1.8 Å, σ-bond coordination can be reasonably proposed. The situation becomes more controversial for values around 1.9–2.0 Å. Higher values up to 2.4 Å are typically the range indicating a significant interaction between a hydrogen and a silicon, values still much shorter than the sum of the van der Waals radii, 3.4 Å. The nature of the silicon substituents is highly important. For electron-withdrawing substituents, the tendency of Si to be hypervalent is favored as a result of a σ*(Si–R) orbital lower in energy. The IHI (interligand hypervalent interaction) analysis developed by Nikonov is nothing more than the direct consequence of this well-known hypervalence property applied to hydrido(silyl) complexes.[16]

Through some selected examples, we will see the need to combine these various techniques to draw the best view of the bonding nature of a silane. Two main classes of compounds will be examined in details. The first section deals with a series of complexes resulting from the activation of disilane compounds, whereas in a second part we will examine the reactivity of ruthenium complexes with monosilane compounds, either primary or secondary silanes.

Disilane Coordination

In view of the fascinating chemistry displayed by the bis(dihydrogen) ruthenium complex $RuH_2(H_2)_2(PCy_3)_2$ (**1**),[17] we were interested to isolate an analogous complex but incorporating two other σ-ligands, silane in place of dihydrogen. This was achieved by using disilane compounds. The chelating effect allowed for the stabilization but was not the determinant factor, as we will detail below. The series of general formula $[RuH_2\{(\eta^2\text{-}HSiMe_2)_2X\}(PCy_3)_2]$ [the spacer X between the two Si atoms contains two or three atoms, X = C_6H_4, $(CH_2)_n$, $OSiMe_2O$] was isolated and fully characterized (Scheme 1).[18] The most relevant data from multinuclear NMR experiments (see Table 1, compounds **2**–**5**) were the following: (i) one triplet near –8 ppm for the σ-Si–H protons and an AA′XX′ resonance near –12 ppm for the two classical hydrides. Coalescence of the two signals was observed at high temperature and an exchange barrier of roughly 65 kJ·mol^{-1} was determined. Deuterium incorporation was equally observed on the two hydride sites implying a rather easy exchange process between the two types of hydrogen atoms. (ii) The $^{29}Si\{^{31}P\}$ INEPT spectra showed a doublet with J_{SiH} values in the range 65–82 Hz, representing a significant reduction from the values for the free disilane (Δ = 106 to 125 Hz) in agreement with a stretching of the Si–H bond as a result of σ-coordination.

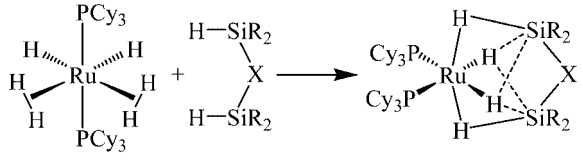

1

Scheme 1. Synthesis of the bis(silane) complexes of general formula $[RuH_2\{(\eta^2\text{-}HSiMe_2)_2X\}(PCy_3)_2]$.

The complexes were characterized by X-ray diffraction, and the measurements at low temperature allowed a very good location of the hydrogen atoms, ascertained by DFT calculations (see below and Table 2). They display the same overall structure, a distorted octahedral with two *cis* phosphane groups (P–Ru–P angle close to 108°) and the disilane ligand bonded to the ruthenium through two σ-Si–H bonds in a *trans* position. Activation of the Si–H bond is illustrated by a significant lengthening compared to the free silane. For example for $[RuH_2\{(\eta^2\text{-}HSiMe_2)_2(C_6H_4)\}(PCy_3)_2]$ (**2**) the two σ-Si–H bond lengths are 1.84(2) Å as determined by X-ray diffraction and 1.848 Å by DFT calculations at the B3LYP level, whereas the Ru–Si distances are close to 2.42 Å by X-ray diffraction or DFT calculations (Table 2, Figure 3). After obtaining the first X-ray structure,[19] we were quite surprised by the *cis* position of the bulky phosphane groups. In fact, no matter the nature of the disilane $[HMe_2Si(X)SiMe_2H$ with X = C_6H_4, $(CH_2)_2$, $OSiMe_2O]$ or the phosphane (PCy_3, PPh_3) coordinated, the same overall geometry was obtained (Table 2).[18] We noted that the distances between the classical hydrides and the silicon atoms were close to 2.2 Å, much shorter than the sum of the van der Waals radii (3.4 Å for hydrogen and silicon). Detailed DFT studies by means of two hybrid functionals B3LYP and B3PW91 gave important information on the coordination mode of the disilane ligand to the ruthenium. Three isomers were characterized on the singlet potential energy surface. As an example, we will concentrate on the three isomeric structures of $[RuH_2\{(\eta^2\text{-}HSiH_2)_2(C_6H_4)\}(PH_3)_2]$. The most stable isomer **A** has a geometry closely resembling that found by X-ray diffraction for **2** (Figure 3). The disilane is symmetrically coordinated to the ruthenium with the two σ-hydrogen atoms almost *trans* to each over (the H–Ru–H angle is 172°). The two Si–H distances of 1.848 Å are identical to the values found by X-ray diffraction. More interesting, the classical hydrides are turned toward the silicon atoms, imposing a *cis* position for the phosphane groups. The distances between the silicon atoms and the hydrides are 2.25 Å, indicative of weak attractive interactions again in excellent agreement with X-ray data. It is worth noting that location of hydrogen atoms in the coordination sphere of a metal has been always subject to debate. Very recently, we have published X-ray and neutron data for the bis(dihydrogen) complex $RuH_2(H_2)_2(PCyp_3)_2$ incorporating two tricyclopentylphosphane li-

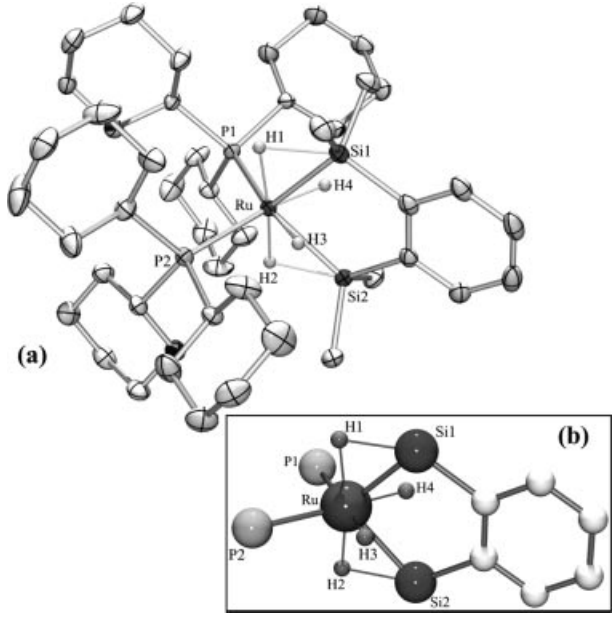

Figure 3. (a) X-ray crystal structure of $[RuH_2\{(\eta^2\text{-}HSiMe_2)_2(C_6H_4)\}(PCy_3)_2]$ (**2**). (b) DFT/B3PW91-optimized geometry of $[RuH_2\{(\eta^2\text{-}HSiH_2)_2(C_6H_4)\}(PH_3)_2]$.

Table 1. Selected NMR and IR [cm^{-1}] data[a] for various silane and silyl ruthenium complexes.

	Formula	δ = ^{1}H [ppm]	J_{SiH} [Hz]	δ = ^{29}Si [ppm]	$\nu_{Ru-H-Si}$	ν_{Ru-H}	Ref.
2	$RuH_2[(\eta^2\text{-}HSiMe_2)_2(C_6H_4)](PCy_3)_2$	–7.74 (t) –12.03 (m)	65	4.8	1778	1969 1985	[16,17]
3a	$RuH_2[(\eta^2\text{-}HSiMe_2)_2(CH_2)_2](PCy_3)_2$	–8.21 (t) –12.65 (m)	70	12.2	1773	1981 2012	[16]
3b	$RuH_2[(\eta^2\text{-}HSiMe_2)_2(CH_2)_2](PCy_3)(PPh_3)$	–7.68 (t) –11.10 (dd) –11.47 (dd)	64	14.7	1768	 1989 2008	[16]
3c	$RuH_2[(\eta^2\text{-}HSiMe_2)_2(CH_2)_2](PPh_3)_2$	–7.60 (t) –10.92 (m)	64	16.4	1797	1961 1978	[16]
4	$RuH_2[(\eta^2\text{-}HSiMe_2)_2(CH_2)_3](PCy_3)_2$	–8.49 (t) –12.17 (m)	75	–11.1	1803	1961 1994	[16]
5	$RuH_2[(\eta^2\text{-}HSiMe_2)_2(OSiMe_2O)](PCy_3)_2$	–9.14 (t) 11.20 (m)	82	4.9	1798	1955 2045	[16]
6	$RuH_2[(\eta^2\text{-}HSiMe_2)_2NH](PCy_3)_2$	–8.36 (br) –8.62 (br) –9.93 (br) –10.76 (br)	–	–	1712	 1972 2040	[13]
7	$RuH_2[(\eta^2\text{-}HSiMe_2)_2O](PCy_3)_2$	–8.1 (br) –8.5 (br) –9.4 (br) –10.2 (br)	22 (av.)[b]	–5.61	1699	 1969 2045	[16,17]
8a	$RuH_2[(\eta^2\text{-}HSiPh_2)_2O](PCy_3)_2$ (sym)	–7.67 (br) –9.70 (t)	41 (av.)[b]	4.80	1670	1976 2019	[16,12]
8b	$RuH_2[(\eta^2\text{-}HSiPh_2)_2O](PCy_3)_2$ (non-sym)	–7.08 (br) –8.11 (br) –8.99 (br. t) –9.81 (br. t)					
9a	$RuH_2[(\eta^2\text{-}HSiPh_2)\text{-}O\text{-}(SiHPh_2)](PPh_3)_3$	–8.97 (dt, 1 H) –9.40 (br. t, 2 H)	35 (av.)[b]	11.7 –21.4 (free)	–	–	[12]
9b	$RuH_2[(\eta^2\text{-}HSiPh_2)\text{-}O\text{-}(Si(OH)Ph_2)](PPh_3)_3$	–9.15 (m, 3 H)	–	–	–	–	[12]
10	$RuH_3(SiCl_2Me)(PPh_3)_3$	–9.76 (m)	39.7 (av.)[b]	36.4	–	1961.5	[19]
11	$RuH_3(SiPyr_3)(PPh_3)_3$	–9.80 (m)	47.4 (av.)[b]	8.6	–	1960 1969	[21]
12a	$RuH_3(SiMe_3)(PMe_3)_3$	–10.18 (br. m)	–	–10.8	–	1887 (av.)	[25]
12b	$RuH_3(SiEt_3)(PMe_3)_3$	–10.53 (br. m)	–	12.7	–	1897 (av.)	[25]
12c	$RuH_3(SiMe_2CH_2SiMe_3)(PMe_3)_3$	–10.15 (br. m)	25	–9.2 –0.9 (free)	–	1898 (av.)	[20]
13	$RuH_2(\eta^2\text{-}HSiPh_3)(\eta^2\text{-}H_2)(PCy_3)_2$	–8.3 (br. s)	18 (av.)[b]	5.7	–	–	[26]
14	$RuH_2(\eta^2\text{-}HSiMe_2Cl)(\eta^2\text{-}H_2)(PCy_3)_2$	–8.51 (br. s)	–	38	–	–	[27]
15	$RuH_2\{\eta^4\text{-}HSiMe_2(CH{=}CHMe)\}(PCy_3)_2$	–8.77 (br.) –9.46 (dt) –12.46 (dt)	105	–11.3	–	1945 2021	[30]
16	$RuCl(H)(\text{-}CH_2SiMe_2)(PMe_3)_3$ (fac)	–7.7 (dt)	75.0	–19.4	1615	–	[31]
	$RuCl(H)(\text{-}CH_2SiMe_2)(PMe_3)_3$ (mer)	–6.0 (dt)	77.5	–19.8	–	–	[31]
17	$RuH(\eta^2\text{-}HSiEt_3)\{(\eta^3\text{-}C_6H_8)PCy_2\}(PCy_3)$	–9.54 (br. t) –12.63 (dd)	36.7 24.7	–	–	–	[36]
18	$RuH(\eta^2\text{-}HSiMe_2Et)\{(\eta^3\text{-}C_6H_8)PCy_2\}(PCy_3)$	–9.45 (ps t) –12.46 (dd)	40.1 24.1	5.0	–	–	[35]
19	$RuH(\eta^2\text{-}HSiMe_2Cl)\{(\eta^3\text{-}C_6H_8)PCy_2\}(PCy_3)$	–9.06 (ps t) –11.98 (dd)	37.3 24.1	46.2	–	–	[27]
20	$Cp^*RuCl(\eta^2\text{-}HSiClMe_2)(P\textit{i}Pr_3)$	–9.65 (t)	33.5	–	1916	–	[33]
21	$[CpRuH(SiCl_3)(PMe_3)_2][B(3,5\text{-}(CF_3)_2C_6H_3)_4]$	–9.87 (t)	48	30.6	–	–	[37]
22a	$Ru_2H_4(\mu\text{-}\eta^2\text{:}\eta^2\text{:}\eta^2\text{:}\eta^2\text{-}SiH_4)(PCy_3)_4$	–6.0 (br.) –8.6 (br.)	36 (av.)[b]	290.2	1667	1911	[38,39]
23	$Ru_2H_2[\mu\text{-}\eta^2\text{:}\eta^2\text{-}H_2Si(OMe)_2]_3(PCy_3)_2$	–9.94 (br.)	22 (av.)[b]	85.7	1703	1899 2022	[39]
24	$[Cp^*RuH]_2(\eta^2\text{:}\eta^2\text{-}H_2Si\textit{t}Bu_2)$	–6.15 (s) –16.63 (s)	75	75.5	1790	–	[40]

Table 1. *(continued)*.

	Formula	δ = ^{1}H [ppm]	J_{SiH} [Hz]	δ = ^{29}Si [ppm]	$\nu_{Ru-H-Si}$	ν_{Ru-H}	Ref.
25a	$[Cp^*Ru(CO)]_2(\eta^2:\eta^2\text{-}H_2SitBu_2)$	–13.60 (s)	22.4	186.2	–	–	[40]
25b	$[Cp^*Ru(CO)]_2(\eta^2:\eta^2\text{-}HSitBu_2)H$	–11.79 (s) –14.40 (s)	31.6	168.2	–	–	[40]
26a	$[Cp^*Ru]_2(\mu\text{-}\eta^2\text{-}HSitBu_2)(\mu\text{-}\eta^2\text{-}HSiPhH)(\mu\text{-}H)H$	–11.64 (s) –12.84 (s) –14.00 (s) –16.46 (s)	26 49 	–	1813 1613	2054	[40]
26b	$[Cp^*Ru]_2(\mu\text{-}\eta^2\text{-}HSitBu_2)(\mu\text{-}\eta^2\text{-}HSiEtH)(\mu\text{-}H)H$	–12.32 (s) –13.26 (s) –14.29 (s) –16.67 (s)	– 	–	1835 1659	2062	[40]

[a] NMR/IR data were obtained under the following conditions: **2**–**5**,**12**,**17**,**23**, C_6D_6, room temp./Nujol mull; **6**,**8**,**9a**,**22**, C_7D_8, 193 K/Nujol mull; **7**, C_7D_8, 178 K/Nujol mull; **9b**,**11**,**13**–**15**,**18**–**19**, C_7D_8, room temp./Nujol mull; **10**, CD_2Cl_2, room temp./KBr; **16**, C_7D_8, 301 K/Fluorolube; **20**, C_7D_8, 233 K/Nujol mull; **21**, CD_2Cl_2, 298 K; **24**–**26**, C_7D_8, 298 K/KBr. [b] J_{SiH} values were determined at room temperature. Average values involving all the hydrides and dihydrogen ligand in the case of **13**.

Table 2. Selected interatomic distances [Å] for various silane and silyl ruthenium complexes.

	Formula	Ru–Si X-ray data	 DFT[a]	Si–H X-ray data	 DFT[a]	Si···H X-ray data	 DFT[a]	Ref.
2	$RuH_2[(\eta^2\text{-}HSiMe_2)_2(C_6H_4)](PCy_3)_2$	2.425(1)	2.425	1.84(2)	1.848	2.22(2) 2.18(2)	2.253 2.253	[16,17]
		2.429(2)	2.425	1.84(2)	1.848	2.12(2) 2.21(2)	2.253 2.253	
3a	$RuH_2[(\eta^2\text{-}HSiMe_2)_2(CH_2)_2](PCy_3)_2$	2.428(1)	2.441	1.73(3)	1.853	2.27(3) 2.13(3)	2.22 2.329	[16]
		2.411(1)	2.441	1.78(3)	1.853	2.12(3) 2.31(3)	2.329 2.22	
5	$RuH_2[(\eta^2\text{-}HSiMe_2)_2(OSiMe_2O)](PCy_3)_2$	2.484(1)	2.451	1.77(4)	1.826	2.25(3) 2.43(3)	2.170 2.484	[16]
		2.434(1)	2.447	1.81(3)	1.839	2.32(3) 2.04(3)	2.426 2.168	
6	$RuH_2[(\eta^2\text{-}HSiMe_2)_2NH](PCy_3)_2$	2.395(2)	2.416	1.93(5)	1.922	2.35(6) 2.25(6)	2.510 2.191	[13]
		2.434(2)	2.490	1.91(5)	1.775	2.39(5) 2.09(6)	2.500 2.367	
9b	$RuH_2[(\eta^2\text{-}HSiPh_2)\text{-}O\text{-}(Si(OH)Ph_2)](PPh_3)_3$	2.356(2)	–	1.97(5)	–	2.03(5) 2.07(5)	–	[12]
10	$RuH_3(SiCl_2Me)(PPh_3)_3$	2.2760(4)	–	–	–	1.86(2) 1.94(2) 1.94(3)	–	[19]
12a	$RuH_3(SiMe_3)(PMe_3)_3$	2.376(1)	–	–	–	2.13(5) 2.18(5) 2.23(5)	–	[25]
12c	$RuH_3(SiMe_2CH_2SiMe_3)(PMe_3)_3$	2.3774(8)	–	–	–	2.00(4) 2.09(4) 2.05(5)	–	[20]
12d	$RuH_2(SiMe_2CH_2CH_2SiMe_2)(PMe_3)_3$	2.4682(9) 2.4514(9)	–	1.81(4)	–	–	–	[20]
13	$RuH_2(\eta^2\text{-}HSiPh_3)(\eta^2\text{-}H_2)(PCy_3)_2$	2.385(2)	2.394	1.72(3)	1.946	1.83(3) 2.40(4)	2.071 2.116	[23]
15	$RuH_2\{\eta^4\text{-}HSiMe_2(CH{=}CHMe)\}(PCy_3)_2$	2.498(2)	2.499	1.59(8)	1.658	–	–	[31]
16	$RuCl(H)(\text{-}CH_2SiMe_2)(PMe_3)_3$ (*fac*)	2.526(2)	–	1.664	–	–	–	[25]
16	$RuCl(H)(\text{-}CH_2SiMe_2)(PMe_3)_3$ (*mer*)	2.468(2)	–	1.557	–	–	–	[25]
18	$RuH(\eta^2\text{-}HSiMe_2Et)\{(\eta^3\text{-}C_6H_8)PCy_2\}(PCy_3)$	2.418(1)	2.468	–	1.847	–	2.164	[35]
19[b]	$RuH(\eta^2\text{-}HSiMe_2Cl)\{(\eta^3\text{-}C_6H_8)PCy_2\}(PCy_3)$	2.353(2)	2.398	1.91 (2)	1.891	1.99(2)	2.076	[27]
20	$Cp^*RuCl(\eta^2\text{-}HSiClMe_2)(PiPr_3)$	2.398(1)	2.427	2.05	2.072	–	–	[33]
21	$[CpRuH(SiCl_3)(PMe_3)_2]^+$	2.329(1)	–	1.77(5)	–	–	–	[37]
22b	$Ru_2H_4(\mu\text{-}\eta^2\text{:}\eta^2\text{:}\eta^2\text{-}SiH_4)(PiPr_3)_4$	2.1875(4)	2.229	1.69(3) 1.73(3)	1.685 1.685	–	–	[39]

Table 2. *(continued)*.

	Formula	Ru–Si X-ray data	Ru–Si DFT[a]	Si–H X-ray data	Si–H DFT[a]	Si···H X-ray data	Si···H DFT[a]	Ref.
23	$Ru_2H_2[\mu\text{-}\eta^2\text{:}\eta^2\text{-}H_2Si(OMe)_2]_3(PCy_3)_2$	2.456(3) 2.364(3) 2.408(3) 2.419(3) 2.355(3) 2.408(3)	2.486 2.398 2.551 2.551 2.400 2.487	–	in the range 1.654–1.760	–	–	[39]

[a] All the calculations were carried out at the B3LYP level of theory, except for compounds **2**, **6** (B3PW91) and **20** (BP86), by using the following model compounds: **2** $RuH_2[(\eta^2\text{-}HSiH_2)_2(C_6H_4)](PH_3)_2$, **3a** $RuH_2[(\eta^2\text{-}HSiH_2)_2(CH_2)_2](PH_3)_2$, **5** $RuH_2[(\eta^2\text{-}HSiH_2)_2(OSiH_2O)](PH_3)_2$, **6** $RuH_2[(\eta^2\text{-}HSiMe_2)_2NH](PCy_3)_2$, **13** $RuH_2(\eta^2\text{-}HSiH_3)(\eta^2\text{-}H_2)(PH_3)_2$, **15** $RuH_2\{\eta^4\text{-}HSiH_2(CH{=}CHMe)\}(PH_3)_2$, **18** $RuH(\eta^2\text{-}HSiMe_3)\{(\eta^3\text{-}C_6H_8)PH_2\}(PH_3)$, **19** $RuH(\eta^2\text{-}HSiMe_2Cl)\{(\eta^3\text{-}C_6H_8)PH_2\}(PH_3)$, **20** $Cp^*RuCl(\eta^2\text{-}HSiClMe_2)(P\mathit{i}Pr_3)$, **22** $Ru_2H_4(\mu\text{-}SiH_4)(PH_3)_4$, **23** $Ru_2H_2(\mu\text{-}H_2Si(OMe)_2)]_3(PH_3)_2$. [b] Data for one isomer.

gands.[15] Additional comparison with DFT values shows that X-ray data are more and more reliable for hydride location, when of course, high quality measurements can be obtained at low temperature. Isomer **B** was optimized as a minimum lying 32 kJ·mol^{-1} above **A**. Isomer **B** has no symmetry whatsoever, and the two Si–H bonds are now very different: one is *trans* to a phosphane whereas the second one is *trans* to a hydride. One more striking difference with isomer **A** is that all the distances between the hydrides and the silicon atoms exceed the sum of the van der Waals radii (3.52 and 3.58 Å). A similar situation is found in isomer **C** with distances between the hydrides and the silicon atoms of 3.42 Å. Isomer **C** is characterized by a *trans* position of the phosphane groups, with the two Si–H bonds being *trans* to a hydride. Thus, **C** displaying an analogous geometry to the bis(dihydrogen) complex **1**, with in particular *trans* phosphane groups and two σ-ligands *trans* to the hydrides, is not the most stable isomer and is in fact 45 kJ·mol^{-1} above **A**. Similar observations were found when using various disilanes with at least two atoms bridging the two Si. Thus, these close H···Si contacts are a stabilizing feature of the overall structure: we call them *SISHA* interactions (*S*econdary *I*nteraction between a *S*ilicon and a *H*ydrogen *A*tom). These SISHA interactions energetically compensate not only the hindered *cis* position of the bulky phosphane groups, but also the disfavored *trans* position of the σ-bonds (back-donation competition).

In the specific case of only one atom between the two Si, as for example in the case of disiloxane or disilazane, the situation is different as a result of a steric constraint upon coordination of the disilane ligand. Indeed, we have recently characterized both by X-ray diffraction and DFT calculations the disilazane complex $[RuH_2\{(\eta^2\text{-}HSiMe_2)_2NH\}(PCy_3)_2]$ (**6**).[20] For the first time the choice of the functional for DFT calculations in silane ruthenium chemistry turned to be crucial. Major differences were observed with the use of B3LYP by comparison to the X-ray data, whereas a very good match was obtained with B3PW91 (Figure 4). The two phosphane groups in **6** are still in a *cis* disposition but the disilazane ligand has now the two Si–H bonds also in a *cis* disposition, similarly to the case of isomer **B** described above. In **2** by X-ray diffraction or **A** by DFT calculations, the four Si···H distances between the hydrides and the silicon atoms were close to 2.2 Å, whereas in **6** they lie between 2.1 and 3.7 Å by X-ray diffraction and 2.2 to 3.9 Å by DFT calculations. It is now interesting to compare the NMR properties of the two complexes. At room temperature, as already pointed out, the ^{1}H NMR spectrum of **2** displays two signals for the two types of hydrogen atoms. Coalescence is observed at much higher temperature. In contrast, in the case of **6**, only one signal is observed at room temperature, whereas decoalescence is achieved at low temperature. The exchange process is thus easier in the case of **6**. In-depth NMR and theoretical studies of the mechanism of the exchange process were undertaken on $[RuH_2\{(\eta^2\text{-}HSiMe_2)_2(C_2H_4)\}(PCy_3)_2]$ (**3a**), a complex very similar to **2** as shown by X-ray, NMR and DFT data.[14] The free energy of activation for exchange is 72 kJ·mol^{-1} at 376 K, and the entropy of activation is close to zero, indicative of an intramolecular process. A complete

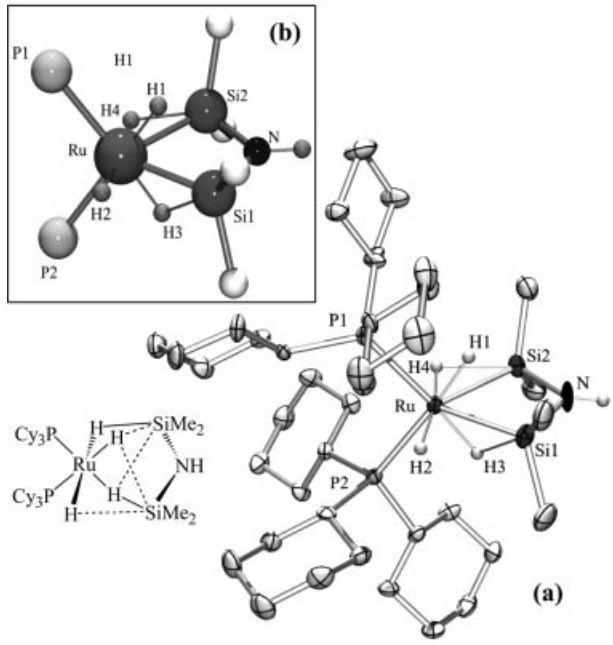

Figure 4. (a) X-ray crystal structure of $[RuH_2\{(\eta^2\text{-}HSiMe_2)_2NH\}(PCy_3)_2]$ (**6**). (b) DFT/B3PW91-optimized geometry of $[RuH_2\{(\eta^2\text{-}HSiMe_2)_2NH\}(PCy_3)_2]$.

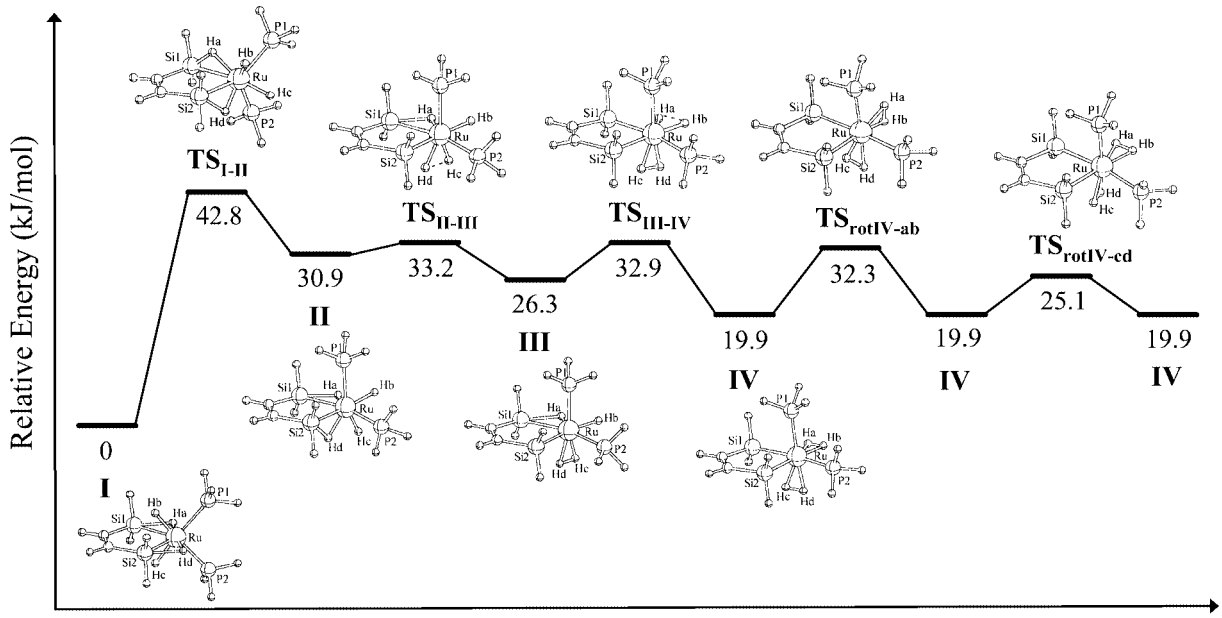

Figure 5. A picture of the intermediates and the transition states involved in the exchange process between the hydrides and the Si–H hydrogen atoms within the model complex $[RuH_2\{(\eta^2\text{-}HSiH_2)_2(C_2H_2)\}(PH_3)_2]$ at the DFT/B3LYP level.

picture of the exchange process deriving from DFT calculations is drawn in Figure 5. Isomer **I** $[RuH_2\{(\eta^2\text{-}HSiH_2)_2(C_2H_2)\}(PH_3)_2]$ was also used as a model complex for **3a**. Exchange of all the different hydrogen atoms can be achieved through the intermediacy of new σ-dihydrogen complexes. Indeed conversion of isomer **I** to the asymmetric isomer **II** in which the SISHA interactions have been broken is the first step. It is then easy to break a Si–H bond. Two hydrogen atoms are now close enough to form a new σ-ligand as in isomer **III**. A similar process with the second Si–H bond leads to isomer **IV** with two dihydrogen ligands. Exchange can now occur via rotation of the dihydrogen ligands and reversal of the isomerisation process. All the transition states connecting the different isomers have been calculated. $\mathbf{TS_{I-II}}$ is the most energetically demanding step. The overall barrier is 42.8 kJ·mol^{-1}. In summary, breaking of the SISHA interactions is responsible for the most energetically demanding step in the exchange process.

Monosilane Coordination

Primary Silanes

A wide variety of monosilanes of the type $HSiR_3$ (R = alkyl, aryl, alkoxy or halogen) reacts with dihydride ruthenium complexes to form the corresponding silane complexes stabilized by various interactions between the hydrides and the silicon atom (see Figure 6).[21–25] Depending on the activation degree of the Si–H bond, they can be interpreted as σ-silane or silyl hydride complexes, namely $RuH_2(\sigma\text{-}HSiR_3)L_2L'$ or $RuH_3(SiR_3)L_2L'$, respectively (L, L′ = PR_3, CO, σ-H_2). The NMR spectroscopic data are very similar for most of the complexes, as can be seen from Table 1. In the case of $RuH_3(SiCl_2Me)(PPh_3)_3$ (**10**) for example,[21] the ^{1}H NMR spectrum exhibits only one hydride resonance at –9.76 ppm with the characteristic AA′A′′XX′X′′ coupling pattern of $MH_3(SiX_3)(PR_3)_3$ complexes arising from the sum of three phosphorus–hydrogen coupling constants, $|^2J_{HPtrans} + 2\ ^2J_{HPcis}|$. The $^1H\{^{31}P\}$ NMR spectrum gives a singlet with ^{29}Si satellites (J_{SiH} = 39.7 Hz) in agreement with a possible σ-silane bonding mode and/or Si···H interactions. The $^{31}P\{^1H\}$ NMR spectrum shows only a singlet at δ = 38.31 ppm, suggesting that the three phosphorus are equivalent on the NMR time scale. This is confirmed by the $^{29}Si\{^1H\}$ DEPT NMR spectrum that exhibits a quadruplet centered at δ = 36.4 ppm ($^2J_{SiP}$ = 12.8 Hz). No decoalescence of the hydride or phosphorus signals was observed even at low temperature, indicative of a fast exchange process in this unsymmetrical compound.

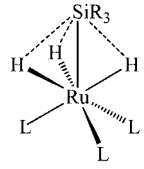

L = phosphane, CO, σ-H_2
R = alkyl, aryl, alkoxy, amino or halogen

Figure 6. Schematic representation of a series of complexes of general formula $RuH_3(SiR_3)L_2L'$.

In the case of symmetrical complexes (C_3 axis), the equivalency of the hydrides prevents any further interpretation regarding the bonding mode. This situation leads to some disagreement on whether or not the $SiPyr_3$ group is rotating in $RuH_3(SiPyr_3)(PPh_3)_3$ (**11**) for example (Pyr = pyrrolyl). Hübler et al. proposed a bonding scheme that allows a facile rotation when considering the contribution represented in Figure 7 (b) to be preponderant.[23] On the

contrary, Nikonov pleads an electron-density transfer from the σ(M–H) bonding orbitals into the σ*(Si–N) antibonding orbitals to be the main contribution, thus leading to a rigid structure (Figure 6 and Figure 7, a).[26] However, Nikonov uses a DFT study reported by Hübler et al. to support his argumentation, but this was actually a MP2 study of an osmium analogue, which is certainly not transposable to the ruthenium case. It is thus difficult to make conclusions on the basis of these experimental and computational data. In the case of the $SiMe_3$ group, Berry et al. observed no dynamic process in $RuH_3(SiMe_3)(PMe_3)_3$ (**12a**) on the NMR time scale (only a slight broadening of the Ru–H resonances at 190 K).[27] In these symmetrical compounds, the presence of a Ru-η^2-H–Si bond (or one strong Si···H interaction) could have led to decoalescence of the hydride signal. However, due to the limited range in temperatures, one cannot conclude on whether the activation energy for the formation/breaking of such interactions would be very low or very high.

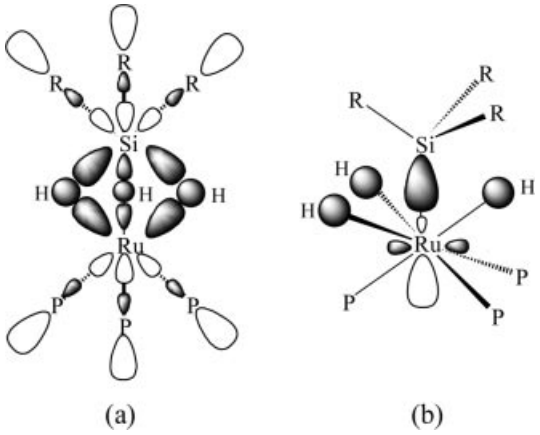

Figure 7. Orbital representation of Ru–H···Si bonding adapted from ref.[19,21]

The fluxionality observed at the NMR time scale for $RuH_3(SiMeCl_2)(PPh_3)_3$,[21] (**10**) but also for $RuH_2(\eta^2\text{-}HSiPh_3)(\eta^2\text{-}H_2)(PCy_3)_2$ (**13**),[28] $RuH_2(\eta^2\text{-}HSiMe_2Cl)(\eta^2\text{-}H_2)(PCy_3)_2$ (**14**),[29] and $RuH_3(SiMe_2CH_2SiMe_3)(PMe_3)_3$ (**12c**),[22] is consistent with exchange processes characterized by low activation energy barriers. In **10** and **12c**, the silane ligand is bearing different substituents (a situation not depicted in Figure 7, a). The presence of different R substituents should affect more or less the balance between the three Si···H interactions in the contribution shown in Figure 7 (a). In **13** and **14**, one phosphane is now replaced by a dihydrogen ligand. It is thus expected a reinforcement of hydride inequivalency. Again, one cannot conclude when no decoalescence of the hydride resonance is observed. NMR spectroscopy can still provide J_{SiH} coupling constants but they are mean values. The interpretation of the raw values has to be done cautiously since the typical ranges for which the Si–H bonds were considered to be either fully activated (< 20 Hz) or just partially elongated (20–70 Hz) have been recently reconsidered.[22,30] The free silane $^1J_{SiH}$ substituent-dependency clearly illustrates the problem. Values vary from 190 Hz in $HSiMe_3$ to 370.6 Hz in $HSiCl_3$ due in part to an increase in the s character in the Si–H bond (Bent's rule). This naturally applies to the J_{SiH} coupling in a complex, more precisely to its two contributions of opposite signs, $^1J_{SiH}$ and $^2J_{SiH}$. The measured J_{SiH} value corresponds to the sum $|^1J_{SiH} + {}^2J_{SiH}|$. In the series of $CpRu(SiR_3)(PR'_3)_2$ complexes, Lemke et al. have shown that an increase in the electron-withdrawing character of the SiR_3 group leads to stronger Ru–Si bonds as monitored by the increase of the $|^2J_{SiP}|$ values.[31] For hydrido(silyl) or σ-silane species with different SiR_3 groups, but considering a similar activation of the Si–H bond, the $|^1J_{SiH}|$ values should increase as a function of the R substituent, with the highest value for the more electronegative group. As an example, coordination of $HSiR_3$ to a metal center leading to 80% activation of the Si–H bond would result to a $|^1J_{SiH}|$ value of 74 Hz for R = Cl and 38 Hz for R = Me. Assuming that the $|^2J_{SiH}|$ values will follow the same trend as the $|^2J_{SiP}|$ values in silyl complexes, the magnitude of the apparent J_{SiH} coupling may not necessarily reflect the silane bonding and its modifications. For example, the apparent J_{SiH} values of 39.7 Hz in $RuH_3(SiMeCl_2)(PPh_3)_3$ (**10**) and 47.4 Hz in $RuH_3(SiPyr_3)(PPh_3)_3$ (**11**) do not necessarily indicate the presence of a σ-silane bond. However, in order to define a trend for the J_{SiH} coupling constants in silane ruthenium complexes, one can start with the coupling constant of 105 Hz measured in the allylsilane complex $RuH_2[\eta^4\text{-}HSiMe_2(CH{=}CHMe)](PCy_3)_2$ (**15**) to give an idea of the upper limit corresponding to an agostic Si–H interaction.[32] We can then consider the *fac* and *mer* isomers of $RuCl(CH_2SiHMe_2)(PMe_3)_3$ described by Berry et al. that reflect a further point on the oxidative addition process (still close to the agostic interaction type).[33] They respectively exhibit J_{SiH} values of 75 and 77.5 Hz associated to Si–H distances of 1.664 Å in the *fac* isomer and 1.557 Å in the *mer* one, in agreement with only slightly elongated Si–H bonds. The next step can be represented by the bis(σ-silane) complexes described in the previous section with coupling constants around 70 Hz. Below that value, it is recommended to interpret the J_{SiH} values with caution, especially when the silicon atom has electron-withdrawing substituents. More information could be now gained thanks to recent improvements in DFT calculations, which allow calculations of J_{SiH} values.[34] Generally, a negative value is the sign of a direct Si–H interaction as $^1J_{SiH}$ are negative due to the negative magnetogyric value of silicon.[35]

Decoalescence of the hydride signal in a polyhydride system is rarely observed. The ^1H NMR spectrum of $RuH_2\{(\eta^2\text{-}HSiPh_2)O(SiHPh_2)\}(PPh_3)_3$ (**9a**) at 203 K, a complex with a dangling Si–H ligand, shows two broad multiplets at –8.97 ppm and –9.40 ppm ($^2J_{HP\,trans}$ = 50 Hz and $^2J_{HP\,cis}$ = 25 Hz) in a 2:1 ratio.[14] At this temperature, the $^{31}P\{^1H\}$ NMR spectrum displays a triplet at δ = 42.62 and a doublet at δ = 38.49 with J_{PP} of 23 Hz. The ^{29}Si-^1H COSY spectrum acquired at 203 K shows a signal corresponding to the dangling Si–H bond (δ –21.4) and another one (δ = 11.7 ppm) correlated to the hydride high-field resonance at δ –8.97 ppm attributed to an (η^2-Si–H) hydrogen.

The fast exchange at room temperature is associated to a J_{SiH} mean value of 35 Hz. Due to line broadening, no J_{SiH} value could be measured at low temperature. According to the above discussion about coupling constants, a definitive assignment between the two formulations, dihydride σ-silane or trihydride silyl with one strong Si···H interaction, is difficult. An X-ray structure of $RuH_2\{(\eta^2\text{-}HSiPh_2)\text{-}O(Si(OH)Ph_2)\}(PPh_3)_3$ (**9b**), resulting from hydrolysis of the dangling Si–H bond of **9a** was obtained. The structure is similar to those described for other $RuH_3(SiR_3)L_3$. The ruthenium is surrounded by the three phosphane groups in a tripodal position with P–Ru–P angles of 103° (av.) and Si–Ru–P angles of 115° (av.). However, one Si–Ru–P angle is 119°, indicating a dissymmetric geometry. The hydrogen atoms were located in the vicinity of the ruthenium at 1.6 Å (av.). The distances between the silicon and the three hydrides are 1.97(5), 2.03(5) and 2.07(5) Å. They are in agreement with an elongated σ-Si–H bond and two SISHA interactions (unfortunately, we have no DFT data for comparison). The Ru–Si distance is 2.356(2) Å, thus at the lower limit of the Ru–Si distances observed in other silane ruthenium complexes. We note that steric hindrance between the phosphane groups and the $OSi(OH)Ph_2$ group may have influenced the bonding. As a matter of fact, there is no decoalescence of the hydride resonance for $RuH_3(SiMe_2CH_2SiMe_3)(PMe_3)_3$ (**12c**) in which the phosphane groups are rather small.[22] In this series of complexes, X-ray data show that the Ru–Si bond lengths range from 2.2760(4) Å in $RuH_3(SiCl_2Me)(PPh_3)_3$ to 2.385(2) Å in $RuH_2(\eta^2\text{-}HSiPh_3)(\eta^2\text{-}H_2)(PCy_3)_2$ (see Table 2). They overlap the distances reported for silyl and σ-silane species and they are mainly in the lower limit region (taking into account the nature of the silicon substituents). In fact, the process of Si–H bond activation can be described similarly to the one proposed for C–H bond activation. Once the proton/metal interaction is established, the Si–M distance decreases while the M–H and Si–H distances stay almost unchanged (until a certain point).[6,36] The main difference comes from the silicon hypervalence that may favor Si···H interactions, keeping the atoms close together in a *cis* position. Lin has discussed this point in a previous review on the structural and bonding characteristics in transition metal–silane complexes.[5] Consequently, a long Ru–Si distance is consistent with an early stage in the activation, i.e. a σ-silane bonding mode, while it remains difficult to conclude for a short one, which appears to be the case in this series. When comparing the Ru–Si distances obtained for this family to the ones measured in the bis(σ-silane) complexes, we deduce that the latter represents an earlier stage in the Si–H bond activation process. This is confirmed by the shorter σ-Si–H bond lengths and the weaker SISHA interactions (longer Si···H distances). For the complexes we are considering here, the SISHA interactions are dedicated to only one silicon atom. This certainly results in a better stabilization of the activated silane and consequently highlights a tight relationship between the Si–H bond activation level and the SISHA interaction strength. The Si–H bond oxidative addition process is better seen as a continuum in energy. SISHA interactions help to equilibrate the electronic density transfers between the ruthenium, the hydrides and the silicon.

The X-ray structure analysis of $RuH_2(\eta^2\text{-}HSiPh_3)(\eta^2\text{-}H_2)(PCy_3)_2$ (**13**) done at 160 K exhibits an elongated σ-Si–H bond [1.72(3) Å] and one strong SISHA interaction [1.843(3) Å]. The remaining hydride is at 2.40(4) Å. This can be related to the nature of the *trans* ligands (PCy_3 and $\sigma\text{-}H_2$) and the steric hindrance as much as the electronic effects can be invoked. The Ru–Si distance [2.385(2) Å] is the longest reported for that series, consistent with a rather early stage in the Si–H bond activation process and one main SISHA interaction. A J_{SiH} value of 18 Hz was recently determined. Considering that five hydrogen atoms are in fast exchange, this observed value is in agreement with the presence of a σ-silane. However the overall geometry was not predictable by NMR spectroscopy, but was confirmed by DFT/B3LYP calculations on the model $RuH_2(\eta^2\text{-}HSiH_3)(\eta^2\text{-}H_2)(PH_3)_2$.[25] The ground state structure shows two SISHA interactions (2.071 and 2.116 Å) and an elongated σ-Si–H (1.946 Å) that is less than 0.2 Å shorter. This short difference is in agreement with the high fluxionality observed by NMR spectroscopy. An analogous study performed on the model $RuH_2(\eta^2\text{-}HSiMe_2Cl)(\eta^2\text{-}H_2)(PH_3)_2$ gives the same results. The location of Cl with respect to the hydrides influences the positioning of the σ-Si–H bond but does not change the energy that much (ΔE = 4.8 kJ/mol between isomers A and B) (see Figure 8 and Table 3). The closest Si···H contact is not in a position *trans* to Cl, as would be predicted for a hydrido(silyl) formulation by using the Nikonov model of interaction, IHI. All the observations are consistent with a σ-bonding mode of the silane.

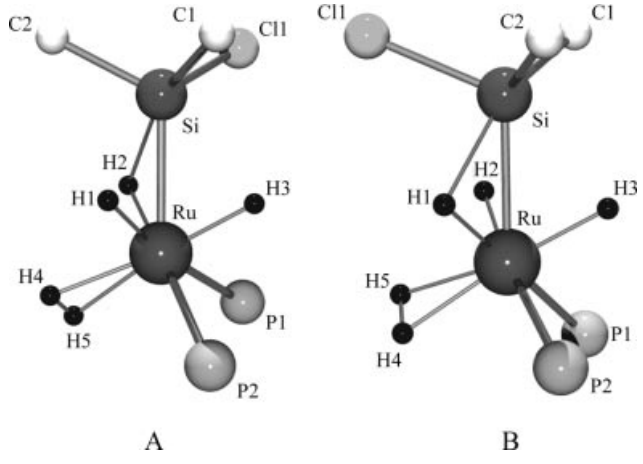

Figure 8. The two DFT/B3LYP-optimized isomeric structures of $RuH_2(\eta^2\text{-}HSiMe_2Cl)(\eta^2\text{-}H_2)(PH_3)_2$.

We undertook a detailed investigation on the complexes $RuH(\eta^2\text{-}HSiR_3)\{(\eta^3\text{-}C_6H_8)PCy_2\}(PCy_3)$ (SiR_3 = $SiEt_3$, $SiMe_2Et$ and $SiMe_2Cl$). In this series, the situation is different because there is no hydride exchange at room temperature, as the result of the presence of two different phosphane groups.[29,37,38] In $RuH(\eta^2\text{-}HSiMe_2Cl)\{(\eta^3\text{-}C_6H_8)PCy_2\}(PCy_3)$ (**19**) for example, the two hydrides resonate at –9.06 ppm (br. t) and –11.98 ppm (dd) and an AB pattern

Table 3. Selected distances [Å] and angles [°] for $RuH_2(\eta^2\text{-}HSiMe_2Cl)(\eta^2\text{-}H_2)(PH_3)_2$ rotamers optimized at the DFT/B3LYP level.

	Rotamer **A**	Rotamer **B**
Ru–P1	2.373	2.371
Ru–P2	2.372	2.375
Ru–Si	2.382	2.387
Si–Cl	2.158	2.145
Si–C	1.892 (C1)	1.893 (C1)
	1.890 (C2)	1.893 (C2)
Ru–H1	1.644	1.637
Ru–H2	1.636	1.633
Ru–H3	1.619	1.627
Ru–H4	1.788	1.808
Ru–H5	1.807	1.786
H4–H5	0.849	0.847
Si–H1	2.091	1.924
Si–H2	1.919	2.076
Si–H3	2.159	2.166
P1–Ru–P2	98.1	97.8
P1–Ru–H1	171.0	178.4
P2–Ru–H2	178.5	173.5
P1–Ru–H3	82.0	84.3
P2–Ru–H3	83.0	83.4
Si–H1–Ru	78.2	83.7
Si–H2–Ru	83.7	79.1
Si–H3–Ru	76.7	76.5
Cl1–Si–H1	153.4	89.0
Cl1–Si–H3	91.3	154.2
C1–Si–H1	90.3	158.0
C1–Si–H2	158.1	86.4
C2–Si–H3	158.3	94.7
H4–Ru–H5	27.3	27.3
Cent(H4,H5)–Ru–H3	176.8	176.6
ΔE [kJ/mol]	0.0	+4.8

(83.9 and 68.8 ppm, J_{PP} = 18.6 Hz) is observed in the $^{31}P\{^1H\}$ spectrum. A 1D HMQC $^{29}Si\text{-}^1H\{^{31}P\}$ experiment shows two doublets in the high-field region with J_{SiH} values of 37.3 and 24.1 Hz (see Figure 9). The coupling of H1 and H2 with silicon are different by more than 10 Hz, but are surprisingly almost the same in the two analogous complexes **17** and **18** with $HSiEt_3$ and $HSiMe_2Et$, respectively (see Table 1). A rather significant change on the Si–H bond activation was expected at least between $HSiMe_2Cl$ and $HSiMe_2Et$ because of the chloride substituent. This point comforts the idea that a direct interpretation of the J_{SiH} value is not appropriate to the description of the bonding mode of the silane. The X-ray structures of the latter two species have been obtained. A partial disorder on the Si substituents could not be solved and the hydrides could only be detected for **19** (see Figure 10). The Si–H distances of 1.91(2) Å (1.891 by DFT calculations) and 1.99(2) Å (2.076 by DFT calculations) can be assigned to an η^2-Si–H and a SISHA interaction, respectively. Even if the values overlap when taking into account the standard deviations, they seem to be in agreement with the corresponding coupling constants. The Ru–Si bond lengths in **18** [2.418(1) Å] and **19** [2.353(2) Å] are clearly different, in agreement with the higher electronegativity of the more tightly bound $SiMe_2Cl$ group. The Ru–Si distances mirror the stability of the silane bonding. As a matter of fact, **19** is stable under an atmospheric pressure of ethylene in toluene, whereas **18** leads to C–Si coupling product and formation of $RuH(\eta^2\text{-}C_2H_4)\{(\eta^3\text{-}C_6H_8)PCy_2\}(PCy_3)$.[37] Compound reactivity is certainly an interesting criterion to differentiate the bonding in this series of silanes. However, what does this shorter Ru–Si bond really mean? The Ru–Si interaction can be strong both in a silyl and in a σ-silane species and increased by the hypervalence tendency of Si. The Ru–Si bond can be shorter thanks to an additional contribution: a bonding overlap between an occupied d(Ru) orbital and empty σ*(Si–R) orbitals. Such a bonding contribution, favored by chloro substituents, has already been used by Lemke et al. to describe a large series of silyl ruthenium complexes.[31] When no d(Ru) orbital is "available", one can consider that the σ(Ru–H) orbital can play the same role. As we have already explained, SISHA interactions help back-donation of electronic density from Ru to Si via the hydrides. This has also been extensively studied by Nikonov et al. but mainly in the particular case of Cl substituents.[16] In summary, the interpretation of the similarities and differences

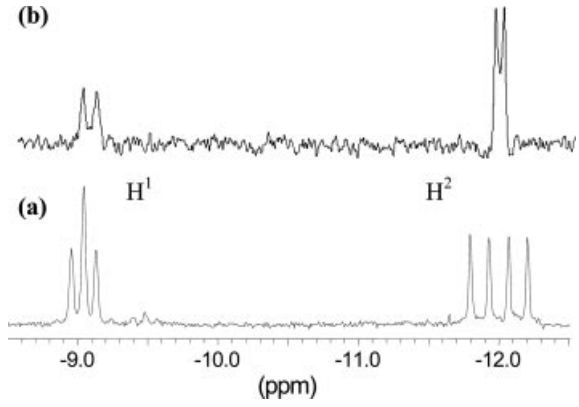

Figure 9. (a) ^1H NMR spectrum (C_6D_6, 400 MHz) and (b) 1D HMQC $^{29}Si\text{-}^1H\text{-}\{^{31}P\}$ in the hydride region of $RuH(\eta^2\text{-}HSiMe_2Cl)\{(\eta^3\text{-}C_6H_8)PCy_2\}(PCy_3)$ (**19**).

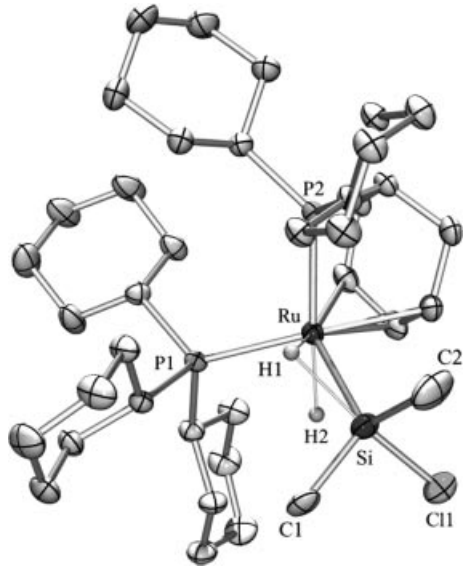

Figure 10. X-ray crystal structure of $RuH(\eta^2\text{-}HSiMe_2Cl)\{(\eta^3\text{-}C_6H_8)PCy_2\}(PCy_3)$ (**19**).

between **18** and **19** is tricky and requires more information. We will publish in due course a full experimental and theoretical study on that series, focusing particularly on the bonding nature of the silane as a function of the chloride number.

It is worth to note that SISHA interactions are not limited to chloride-containing silanes as they clearly appear in most of the examples presented above. But Cl seems to favor secondary interactions as illustrated by the work of Nikonov et al. Cp*RuCl(η^2-HSiMe$_2$Cl)(P*i*Pr$_3$) (**20**) is defined as a σ-silane complex on the basis of experimental and theoretical data (see Figure 11 and Table 1, Table 2).[35] Its X-ray structure exhibits an unusual interaction between the Cl ligand and the silicon atom [$d_{Cl\cdots Si}$ = 3.014(1) Å and the sum of the van der Waals radii is 3.81 Å]. This is well reproduced by DFT calculations on the model CpRuCl(η^2-HSiMe$_2$Cl)(PMe$_3$). The ground state corresponds to the X-ray structure, i.e. the chloride substituent on the silicon is almost "*trans*" to the chloride [Cl–Si···Cl = 165.61(3)°]. The rotamer with a methyl group in "*trans*" is 10.5 kJ/mol less stable and the Si···Cl distance is elongated by about 0.2 Å. This confirms the stabilizing role played by the chloride as it is more electron-withdrawing than the methyl group. A small elongation of the Si–R bond "*trans*" to the secondary interaction is always reported, in agreement with the implication of the σ*(Si–R). In this example, the Si–H bond is absolutely not in the same plane as the Cl substituent which is the case in several silyl hydrido complexes with IHI described by Nikonov et al. Here, the compound is a "real" σ-silane complex. In the absence of any other hydride, further stabilization can only be gained by the formation of a secondary interaction between Si and Ru–Cl. Such an interaction is maximized for a Ru–Cl not orientated *trans* to Si–H. As discussed above, a similar situation has been observed when considering the RuH$_2$(η^2-HSiMe$_2$Cl)(η^2-H$_2$)(PH$_3$)$_2$ rotamers.

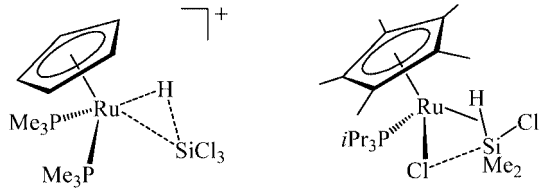

21 **20**

Figure 11. Schematic view of Cp*RuCl(η^2-HSiMe$_2$Cl)(P*i*Pr$_3$) (**20**) and [CpRu(η^2-HSiCl$_3$)(PMe$_3$)$_2$]$^+$ (**21**).

Lemke et al. reported the full characterization of the cationic complex [CpRu(η^2-HSiCl$_3$)(PMe$_3$)$_2$]$^+$ (**21**) formed by protonation of the silyl complex CpRu(SiCl$_3$)(PMe$_3$)$_2$.[39] Compound **21** was formulated as a σ-silane species on the basis of X-ray diffraction and NMR spectroscopic data (see Figure 11). The silane ligand was characterized by a Si–H bond length of 1.77(5) Å in the typical range for σ-silane ligands. The J_{SiH} value of 48 Hz is also in the range expected for a σ-coordination. However, comparison with the corresponding value for the free silane HSiCl$_3$ (370 Hz) denotes a very strong reduction in the Si–H interaction. NMR spectroscopic data also indicate some fluxionality of the silane with respect to its orientation with the two phosphane ligands. The authors associate their data to a σ-silane arrested in its oxidative addition to the ruthenium center indicative of a latter stage of such a process. The geometry can be described as a "three- or four-legged piano stool" depending on how the HSiCl$_3$ ligand is considered. This appears to be in agreement with the measured Si–H distance, only if we analyze this strong interaction to be the consequence of the silicon hypervalence enhanced by the chloro substituents. This is a perfect example to highlight the crucial role of silicon hypervalency on silane bonding.

Secondary Silane

The next step in our silane studies was to examine the reactivity of the bis(dihydrogen) complex **1** with dihydrogenosilanes. We mentioned in the introduction the complexity of silane activation toward σ-coordination as compared to dihydrogen activation. Steric and electronic effects of the Si substituents can tune the σ-coordination as well as the hypervalence properties of the silicon. But one can also face redistribution reactions. Indeed, by adding dihydrogenosilanes to **1**, several silanes were generated in situ. For example, when starting with H$_2$SiMePh, HSiMe$_2$Ph and HSiMePh$_2$ were formed and remained in solution whereas formation of SiH$_4$ and HSiPh$_3$ resulted in their coordination to a metal fragment to produce the corresponding complexes [Ru$_2$H$_4$(μ-η^2:η^2:η^2-SiH$_4$)(PCy$_3$)$_4$] (**22**) and [RuH$_2$(η^2-H$_2$)(η^2-HSiPh$_3$)(PCy$_3$)$_2$] (**13**) (Scheme 2).[40,41] Compound **22** is a unique example of a SiH$_4$ ligand in a bridging position. It is coordinated to two Ru through four σ-Si–H bonds. Each σ-bond [d_{Si-H} = 1.69(3) Å and 1.73(3) Å by X-ray diffraction and 1.685 Å by DFT calculations] is the result of a σ-donation to an empty d orbital of one ruthenium and backbonding from the occupied d orbital of *the other* ruthenium into the σ*(Si–H) antibonding orbital. Interestingly, **22** is characterized by a fast exchange process as the eight hydrogen atoms (four hydrides and four involved in the σ-Si–H bonds) gave a nonet in the ^{29}Si INEPT spectrum with an average J_{SiH} value of 36 Hz. The ^{1}H NMR spectrum displayed one signal in the hydride region at room temperature, but decoalescence into two signals of equal intensity was obtained at 203 K characterized by a low barrier of 36 kJ·mol^{-1}. Another redistribution process was observed by adding an excess of HSi(OMe)$_3$ to **22** (Scheme 2). Formation of Si(OMe)$_4$ and of a new dinuclear complex [Ru$_2$H$_2$(μ–η^2:η^2-H$_2$Si(OMe)$_2$)$_3$(PCy$_3$)$_2$] (**23**) was obtained. Compound **23** represents a very interesting case, illustrating the difficulty in assigning a defined structure in such highly delocalized species. Again eight hydrogen atoms in fast exchange are detected by multinuclear NMR studies with an average J_{SiH} value of 22 Hz. Location of the hydrides was not possible by X-ray diffraction and the proposed formulation was deduced in particular from DFT studies (see Figure 12) and correlated to NMR spectroscopic data. In the model complex [Ru$_2$H$_2$(μ-H$_2$Si(OMe)$_2$)$_3$(PH$_3$)$_2$], one bridging H$_2$Si(OMe)$_2$ ligand is symmetrically coordinated to the two Ru with rather long Ru–

Si distances (2.551 Å) and short Si–H distances (1.653 Å) whereas the two other ligands are dissymetrically bonded to the ruthenium but with shorter Ru–Si distances (2.40 and 2.49 Å) and longer Si–H distances (1.74 and 1.76 Å). The Wiberg bond indices obtained from a natural bond orbital analysis are also in agreement with a different level of activation within the three ligands.

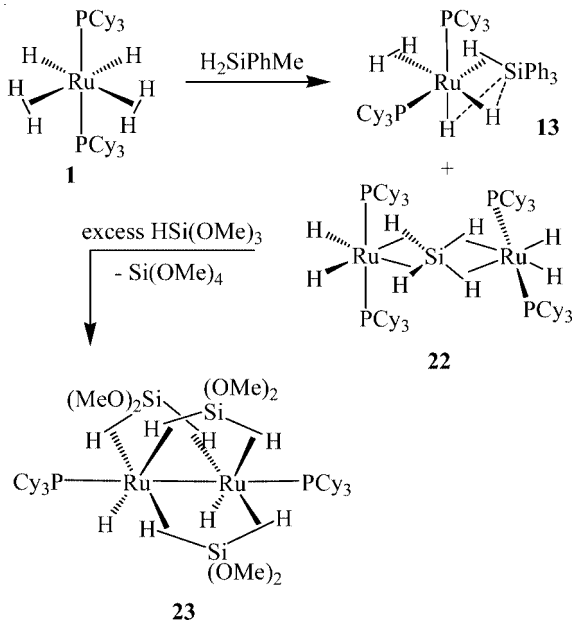

Scheme 2. Redistribution at silicon.

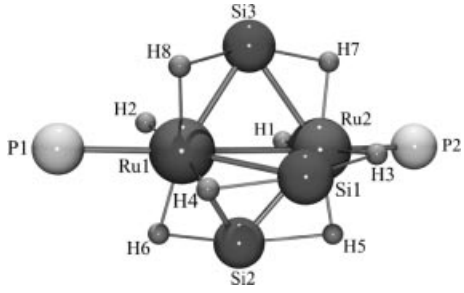

Figure 12. DFT/B3LYP-optimized structure of $[Ru_2H_2(\mu\text{-}H_2Si(OMe)_2)_3(PH_3)_2]$.

An elegant study concerning the synthesis of dinuclear silane ruthenium complexes was reported by Suzuki et al.[42] The mono(silane) complex $[Cp^*Ru(\mu\text{-}H)]_2(\mu\text{-}\eta^2\text{:}\eta^2\text{-}H_2Si\textit{t}Bu_2)$ (**24**) was obtained by reacting $H_2Si\textit{t}Bu_2$ with the ruthenium tetrahydride complex $Cp^*Ru(\mu\text{-}H)_4Cp^*Ru$ (see Scheme 3). The fluxionality observed by NMR at room temperature for the two types of hydrogen was blocked at 153 K resulting in the formation of two signals. The signal at –6.15 ppm displaying a coupling constant of 75 Hz was thus assigned to the σ-ligands, whereas the signal at –16.63 ppm was assigned to the bridging hydrides. The broad adsorption in the IR spectrum at 1790 cm^{-1} (confirmed by deuterium labeling) was also in agreement with σ-silane coordination. Reaction of (**24**) with CO yields a mixture of two new σ-complexes $[Cp^*Ru(CO)]_2(\mu\text{-}\eta^2\text{:}\eta^2\text{-}H_2Si\textit{t}Bu_2)$ (**25a**) and $[Cp^*Ru(CO)]_2(\mu\text{-}\eta^2\text{-}HSi\textit{t}Bu_2)H$ (**25b**). The X-ray structure of **25a** shows long Ru–Si bonds [2.447(1) Å and 2.457(1) Å] and two Si–H bond lengths of 1.77(3) Å and 1.75(3) Å in agreement with two σ-Si–H bonds. (**25a**) is in equilibrium in solution with **25b**. When compound **24** was treated with H_3SiPh or H_2SiEt_2 the corresponding mixed-bridge complexes were obtained, $[Cp^*Ru]_2(\mu\text{-}\eta^2\text{-}HSi\textit{t}Bu_2)(\mu\text{-}\eta^2\text{-}HSiPhH)(\mu\text{-}H)H$ (**26a**) and $[Cp^*Ru]_2(\mu\text{-}\eta^2\text{-}HSi\textit{t}Bu_2)(\mu\text{-}\eta^2\text{-}HSiEtH)(\mu\text{-}H)H$ (**26b**), respectively. Again the σ-Si–H bonds are characterized by long Ru–Si bond lengths.

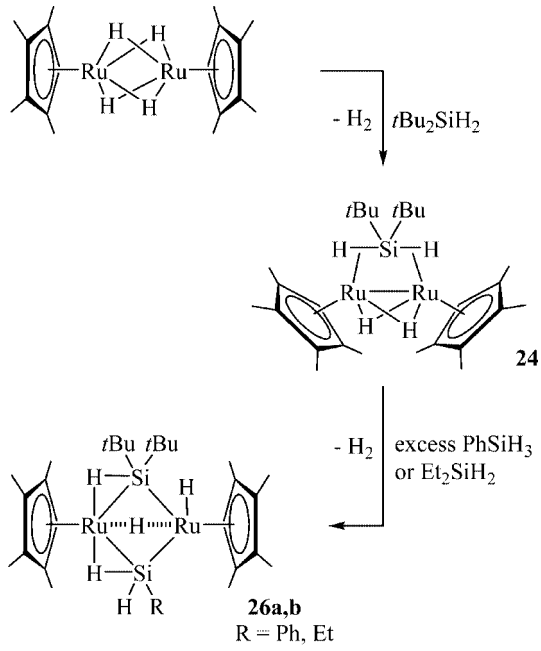

Scheme 3. Synthesis of diruthenium complexes containing μ-silane ligands.

Conclusions

Much work has been published in the area of catalytic silane activation by metal complexes as a wide variety of valuable substrates can be produced. No matter the catalytic process in consideration, one of the main important goal remains selectivity control. This can be achieved by a knowledge of the different key steps occurring in a catalytic cycle. Silane activation by the metal complex is one of these key steps. Throughout all the examples we have considered, it is clear that it is difficult to control this activation process. A continuum exists between the two extremes leading either to σ-silane coordination or oxidative addition. There is no doubt that the tendency of silicon to be hypervalent favors such a continuum, by creating secondary interactions as described above (SISHA interactions).

None of the useful criteria i.e. J_{SiH}, IR bands, d_{Si-H} and d_{Ru-Si} by X-ray diffraction or DFT calculations, can be used *alone* to evaluate the degree of silane activation. In particular, it appears that the interpretation of J_{SiH} values can be difficult, especially for systems including electron-withdrawing substituents and showing fluxional behavior.

The lower limit of 20 Hz used by several authors (including us) should now be set up to 65 Hz for a secure criterion of a σ-Si–H bond. Observation of a broad and intense IR band in the range 1650–1800 cm^{-1} remains a good indication of σ-coordination. When X-ray data involving hydrogen atoms can be supported by DFT calculations, one can considered that a $d_{Si–H}$ value around 1.7–1.8 Å will support the formation of a σ-silane complex. Moreover, silicon-hydrogen distances around 1.9–2.4 Å should alert the researchers of the presence of secondary interactions. The Ru–Si bond strength depends significantly on the silicon-attached substituents, but a short bond length will be consistent with an advanced oxidative addition process.

We have shown that σ-Si–H bonds and SISHA interactions play a major role in alkyl and chloro silane catalytic activation.[29,32,38,43] Moreover, in 2002 we proposed a σ-bond metathesis mechanism which offers alternatives that are distinct from the standard σ-bond metathesis mechanisms and the oxidative addition pathways.[14,44] Successive formation of σ-bonds and secondary interactions (see Scheme 4) allow operating at constant oxidation state whereas oxidative addition/reductive elimination mechanisms change oxidation states by two units. More work is needed both at the stoichiometric and catalytic level to examine the relevance of these types of bonding (σ-Si–H bonds and SISHA interactions) in various catalytic systems with the main goal to achieve better selectivity.

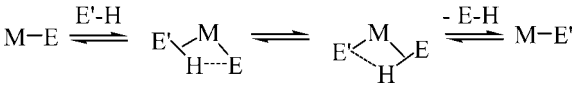

Scheme 4. Functionalization assisted by σ-ligand substitutions and secondary interactions.

Acknowledgments

The CNRS is gratefully acknowledged for financial support of this work. S. S.-E. warmly thanks all her co-workers and colleagues for their contribution to the work presented in this review.

[1] G. J. Kubas, *Metal Dihydrogen and σ-Bond Complexes*, Kluwer Academic/Plenum Publishers, New York, **2001**.
[2] M. A. Esteruelas, L. A. Oro, *Chem. Rev.* **1998**, *98*, 577–588.
[3] G. S. McGrady, G. Guilera, *Chem. Soc. Rev.* **2003**, *32*, 383–392.
[4] J. Y. Corey, J. Braddock-Wilking, *Chem. Rev.* **1999**, *99*, 175–292.
[5] Z. Lin, *Chem. Soc. Rev.* **2002**, *31*, 239–245.
[6] U. Schubert, *Adv. Organomet. Chem.* **1990**, *30*, 151–187.
[7] S. Lachaize, K. Essalah, V. Montiel-Palma, L. Vendier, B. Chaudret, J.-C. Barthelat, S. Sabo-Etienne, *Organometallics* **2005**, *24*, 2935–2943.
[8] C. Hall, R. N. Perutz, *Chem. Rev.* **1996**, *96*, 3125–3146.
[9] D. J. Lawes, S. Geftakis, G. E. Ball, *J. Am. Chem. Soc.* **2005**, *127*, 4134–4135.
[10] R. J. P. Corriu, *J. Organomet. Chem.* **1990**, *400*, 81–106.
[11] R. F. W. Bader, C. F. Matta, F. Cortés-Guzmán, *Organometallics* **2004**, *23*, 6253–6263.
[12] B. Marciniec, *Coord. Chem. Rev.* **2005**, *249*, 2374–2390.
[13] G. J. Kubas, *Catal. Lett.* **2005**, *104*, 79–101.
[14] I. Atheaux, F. Delpech, B. Donnadieu, S. Sabo-Etienne, B. Chaudret, K. Hussein, J. C. Barthelat, T. Braun, S. B. Duckett, R. N. Perutz, *Organometallics* **2002**, *21*, 5347–5357.
[15] M. Grellier, L. Vendier, B. Chaudret, A. Albinati, S. Rizzato, S. Mason, S. Sabo-Etienne, *J. Am. Chem. Soc.* **2005**, *127*, 17592–17593.
[16] G. I. Nikonov, *J. Organomet. Chem.* **2001**, *635*, 24–36.
[17] S. Sabo-Etienne, B. Chaudret, *Coord. Chem. Rev.* **1998**, *178–180*, 381–407.
[18] F. Delpech, S. Sabo-Etienne, J. C. Daran, B. Chaudret, K. Hussein, C. J. Marsden, J. C. Barthelat, *J. Am. Chem. Soc.* **1999**, *121*, 6668–6682.
[19] F. Delpech, S. Sabo-Etienne, B. Chaudret, J.-C. Daran, *J. Am. Chem. Soc.* **1997**, *119*, 3167–3168.
[20] T. Ayed, J.-C. Barthelat, B. Tangour, C. Pradère, B. Donnadieu, M. Grellier, S. Sabo-Etienne, *Organometallics* **2005**, *24*, 3824–3826.
[21] N. M. Yardy, F. R. Lemke, L. Brammer, *Organometallics* **2001**, *20*, 5670–5674.
[22] V. K. Dioumaev, B. R. Yoo, L. J. Procopio, P. J. Carroll, D. H. Berry, *J. Am. Chem. Soc.* **2003**, *125*, 8936–8948.
[23] K. Hübler, U. Hübler, W. R. Roper, P. Schwerdtfeger, L. J. Wright, *Chem. Eur. J.* **1997**, *3*, 1608–1616.
[24] M. Mohlen, C. E. F. Rickard, W. R. Roper, D. M. Salter, L. J. Wright, *J. Organomet. Chem.* **2000**, *593–594*, 458–464.
[25] K. Hussein, C. J. Marsden, J. C. Barthelat, V. Rodriguez, S. Conejero, S. Sabo-Etienne, B. Donnadieu, B. Chaudret, *Chem. Commun.* **1999**, 1315–1316.
[26] G. I. Nikonov, *Angew. Chem. Int. Ed.* **2001**, *40*, 3353–3355.
[27] V. K. Dioumaev, L. J. Procopio, P. J. Carroll, D. H. Berry, *J. Am. Chem. Soc.* **2003**, *125*, 8043–8058.
[28] S. Sabo-Etienne, M. Hernandez, G. Chung, B. Chaudret, *New J. Chem.* **1994**, *18*, 175–177.
[29] S. Lachaize, S. Sabo-Etienne, B. Donnadieu, B. Chaudret, *Chem. Commun.* **2003**, 214–215.
[30] S. R. Dubberley, S. K. Ignatov, N. H. Rees, A. G. Razuvaev, P. Mountford, G. I. Nikonov, *J. Am. Chem. Soc.* **2003**, *125*, 642–643.
[31] S. T. N. Freeman, J. L. Petersen, F. R. Lemke, *Organometallics* **2004**, *23*, 1153–1156.
[32] F. Delpech, S. Sabo-Etienne, B. Donnadieu, B. Chaudret, *Organometallics* **1998**, *17*, 4926 –4928.
[33] V. K. Dioumaev, P. J. Carroll, D. H. Berry, *Angew. Chem. Int. Ed.* **2003**, *42*, 3947–3949.
[34] D. L. Lichtenberger, *Organometallics* **2003**, *22*, 1599–1602.
[35] A. L. Osipov, S. F. Vyboishchikov, K. Y. Dorogov, L. G. Kuzmina, J. A. K. Howard, D. A. Lemenovskii, G. I. Nikonov, *Chem. Commun.* **2005**, 3349–3351.
[36] R. H. Crabtree, *Angew. Chem. Int. Ed. Engl.* **1993**, *32*, 789–805.
[37] S. Lachaize, Ph. D. Thesis, Université Toulouse III – Paul Sabatier (France), **2004**.
[38] M. L. Christ, S. Sabo-Etienne, B. Chaudret, *Organometallics* **1995**, *14*, 1082–1084.
[39] S. T. N. Freeman, F. R. Lemke, L. Brammer, *Organometallics* **2002**, *21*, 2030–2032.
[40] I. Atheaux, B. Donnadieu, V. Rodriguez, S. Sabo-Etienne, B. Chaudret, K. Hussein, J. C. Barthelat, *J. Am. Chem. Soc.* **2000**, *122*, 5664–5665.
[41] R. Ben Said, K. Hussein, J.-C. Barthelat, I. Atheaux, S. Sabo-Etienne, M. Grellier, B. Donnadieu, B. Chaudret, *Dalton Trans.* **2003**, 4139–4146.
[42] T. Takao, S. Yoshida, H. Suzuki, M. Tanaka, *Organometallics* **1995**, *14*, 3855–3868.
[43] F. Delpech, J. Mansas, H. Leuser, S. Sabo-Etienne, B. Chaudret, *Organometallics* **2000**, *19*, 5750–5757.
[44] R. N. Perutz, S. Sabo-Etienne, *Angew. Chem. Int. Ed.*, paper to be submitted.

Received: February 21, 2006
Published Online: April 21, 2006

